

# Electrochemical Dissolution and Passivation of Cu-Ni Alloys in Sodium Sulphate Aqueous Solution

Ayman M. Zaky

Chemistry Department, Faculty of Science, South Valley University, Qena 83523, Egypt  
\*Corresponding Author: azakyl@yahoo.com

Copyright © 2013 Horizon Research Publishing All rights reserved.

**Abstract** The electrochemical behaviour of two copper-nickel alloys is studied in 0.1 M Na<sub>2</sub>SO<sub>4</sub> using cyclic voltammetry, potentiodynamic and current time transient techniques. The microstructure of the compounds formed during anodic sweep is characterized using x-ray diffraction analysis. The forward sweep is characterized by the existence of two well-defined potential regions; the selective dissolution and the simultaneous dissolution potential regions. The first potential region consisted in two anodic peaks A<sub>1</sub> and A<sub>2</sub> corresponding to the formation of Ni(OH)<sub>2</sub> and NiO, and Cu<sub>2</sub>O, respectively. The second potential region consisted in two anodic peaks A<sub>3</sub> and A<sub>4</sub> corresponding to the formation of CuO and Ni<sub>2</sub>O<sub>3</sub>, respectively. It is found that the Cu-Ni system in sulphate solution follows the dissolution-redeposition mechanism of the dissolution of metals from the alloys. The X-ray diffraction analysis confirmed the existence Ni<sub>2</sub>O<sub>3</sub> and CuO on the electrode surface of nickel rich alloy polarized to potential more noble than the potential of A<sub>4</sub> and the existence of Cu<sub>2</sub>O and NiO on the surface of copper-rich alloy polarized to a potential in the A<sub>2</sub> region. Atomic Force microscope images show surface enlargement beyond the critical potential E<sub>crit</sub>.

**Keywords** Copper-nickel, sulphate, cyclic voltammetry, potentiodynamic, current transient, SEM

## 1. Introduction

The copper-nickel system is an isomorphous one in which only a single type of crystal structure is observed for all ratios of the components [1]. Many studies have been conducted of the dealloying of copper-based alloys. The electrochemical behavior of Cu-Ni alloys has been studied by numerous authors in alkaline solutions [2-7]. It was established that the passivity of arrangement of Cu-Ni alloys in 0.1M KOH solution was due to oxide film growth by migration under a high electric field. The rate-controlling parameters were a function of the copper content of the alloy, but largely followed the kinetics of film growth of

pure nickel. Analysis by Auger electron spectroscopy of the formed anodic films indicates that the oxide film is predominantly nickel oxide even when the Cu content in the alloy is 70%, suggesting that Cu in the alloy does not affect the film growth process to any significant extent.

The passive layer formed potentiostatically in 1.0 M NaOH on Cu-50 wt-%Ni has also been investigated, using X-ray photoelectron spectroscopy (XPS) and ion scattering spectroscopy (ISS) [6]. The thickness and the composition of the sublayers of the passive film, as well as the composition of the underlying metal surface, were found to depend on electrochemical parameters such as potential and time of passivation.

Copper-nickel alloy [1] is an amorphous system where copper and nickel forms one single phase all over the range of composition. Two mechanisms of dissolution are generally proposed for the dissolution of metals from isomorphous alloys: simultaneous dissolution of both components of the alloy followed by redeposition of one component on the surface and selective dissolution of one element from the crystal lattice. Three mechanisms are proposed for the dissolution of metals from alloys below their critical potential E<sub>crit</sub>. For a binary alloy AB, below its critical potential, removal of the less noble component B occurs where the more noble component A is present as a layer that covers the alloy surface, which is then ceased any further removal of the less noble component and the current decays to a very low value and is termed the passivation current density i<sub>pass</sub>. As soon as the critical potential of the alloy is reached, the surface loses its planarity and the current rises sharply to a very high value where both components dissolve simultaneously. The ionization-redeposition mechanism assumes an initial simultaneous ionization of both components A and B. This step may involve intermediate formation of ad-atoms of the less noble component, B. Alternatively; direct transfer of B ions from kink sites to the electrolyte solution must be considered [9, 10]. Irrespective of these details of the initial charge transfer step, the electropositive component A is thought to redeposit on the alloy surface in a consecutive step. It is assumed that an ions may be dissolved from the alloy at underpotentials that are cathodic with respect to the reversible potential E<sub>A'</sub>

that agglomerates on the electrode surface. They have, therefore, the character of an unstable intermediate species and will be plated out on the surface of A' crystals at the same electrode potential.

The volume diffusion mechanism, which was introduced by Pickering and Wagner [11], does not consider an "under potential dissolution" of the electropositive component. Instead, the atoms of the latter are assumed to accumulate as mobile ad-atoms on the electrode surface. It may be expected, therefore, that these ad-atoms will have an increasing tendency to move back to the kink sites and steps and to block any further removal of the less noble component from these positions by the usual mechanism of the metal dissolution. Provided that the anodic over potential is high enough, there is, however, an alternative possibility that the preferential dissolution will proceed from terrace sites (which may be in the vicinity of the kink sites [12]). This process results in the formation of surface vacancies. The major concept of the volume diffusion mechanism is that by the injection of these surface vacancies into the bulk of the alloy, a large vacancy super saturation is developed adjacent to the alloy /electrolyte interface which enhances the diffusivity beyond its thermal value. Repopulating of the electrode surface with Cu atoms via volume diffusion is therefore considered to be possible even at room temperature.

The surface diffusion mechanism considers the nucleation and growth of the crystals of the pure, or almost pure, noble component via a surface diffusion process. Following earlier suggestions by Gerischer [13], this mechanism may be described in detail by a model which, for a binary AB, includes:

1. Removal of both components from steps kink sites and formation of ad-atoms of the more noble component A at electrode potentials  $E < E_C$ . The ad-atoms may subsequently (a) crystallize via surface diffusion or (b) accumulate at the steps and kink positions, where they are thought to block the removal of the less noble species. However, in contrast to the assumptions that were made with the volume diffusion process, a small but finite steady-state dissolution rate of B atoms is now considered to be possible by exchange of places between A and B atoms.

2. Removal of B atoms from terrace sites in order to account for the increased dissolution rate at  $E > E_C$ . Since the remaining an atom is expected to form a porous layer of small individual crystallites, this process is thought to operate without transport of B atoms to the electrode surface via volume diffusion.

This present work has used two alloys of different compositions, one being copper rich and the other nickel rich, to elucidate the mechanism of dissolution and the composition of the passive films formed in the Cu-Ni system in 0.1MNa<sub>2</sub>SO<sub>4</sub> solution. The voltammetric profiles of pure copper and pure nickel were included for comparison. The microstructure and composition of the passive film formed during the anodic sweep was characterized by X-ray diffraction analysis. Atomic force

microscopy(AFM) was used to examine the alloy surface for surface enlargement associated with the electric field beyond the critical potential  $E_{crit}$ .

**Table 1.** Composition of the studied alloys

No.	Name	Composition %	
		Cu	Ni
1	Alloy I	80	20
2	Alloy II	20	80

## 2. Experimental

Pure copper and nickel (supplied by Merck 99.99%) and two copper-nickel alloys of the composition Cu-20 wt% Ni and Cu-80 wt% Ni were used in studying the voltammetric behaviour copper-nickel alloys in aerated Na<sub>2</sub>SO<sub>4</sub> solution. The alloys were made by fusion of pure two metals in a graphite crucible at a desired temperature, air cooled and scraped into the desired thickness area. The electrodes were then mounted in a Teflon mount so as only their cross sectional areas were exposed to solution. Before each experiment, the electrodes were mechanically polished starting with fine grained emery papers and followed with alumina paste to obtain a mirror-like electrode surface, then rinsed with acetone and doubly distilled water. Measurements were performed in Na<sub>2</sub>SO<sub>4</sub> solutions prepared from Analar grade chemicals and used without further purification. A conventional electrochemical cell of 100 cm capacity was used for the present work. It was contained three separated compartments two of them were used for fitting both the working and the platinum counter electrodes. The third compartment was used for fitting the reference electrode, which is saturated calomel electrode (SCE).

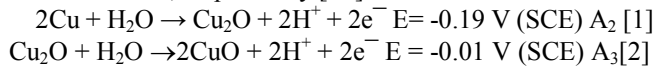
Cyclic voltammetric, potentiodynamic anodic polarization and potentiostatic current/time measurements were carried out with the help of an EG&G potentiostat/Galvanostat Model 237A controlled by a PC computer using 352 corrosion software.

Morphology of the alloy surface in the potential range beyond the critical potential  $E_{crit}$  was maintained by scanning electron micrographs SEM), model XL-200 Philips operated at 15 k eV. The composition of the corrosion products formed during anodic polarization over the alloys surfaces was studied using x-ray diffraction analysis using Philips P. W. Model 1730 diffractometer adopted at 40 kV and 25 mA with Cu- $k_{\alpha}$  radiation and a Ni filter.

## 3. Results and Discussion

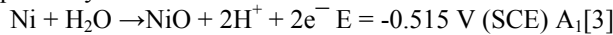
The electrochemical behaviour of the alloys I and II was studied in 0.1 M Na<sub>2</sub>SO<sub>4</sub> between  $E_c = -1600$  mV up to  $E_a = 200$  mV and 1000 mV, respectively with sweep rate of 50 mV s<sup>-1</sup> and the data is represented graphically in Figure 1. The curves of pure copper and pure nickel were introduced

for comparison. The electrochemical behaviour of pure copper, Fig. 1 (curve 1), studied between  $E_c = -1600$  mV and  $E_a = 200$  mV and was characterized by the appearance of two anodic peaks  $A_2$  and  $A_3$ , and two cathodic peaks  $C_2$  and  $C_3$ . The anodic peaks  $A_2$  and  $A_3$  are related to the formation of  $\text{Cu}_2\text{O}$  and  $\text{CuO}$ , respectively [14].

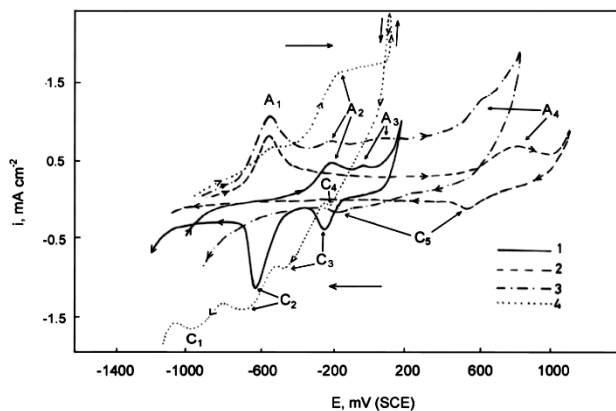


At the same time, the existence of the cathodic peaks  $C_2$  and  $C_3$  was ascribed to the reduction of  $\text{Cu}_2\text{O}$  to  $\text{Cu}$  and  $\text{CuO}$  to  $\text{Cu}_2\text{O}$ , respectively.

Figure 1, curve 2, represents the cyclic voltammetric behaviour of pure nickel [14] studied between  $E_c = -1600$  mV and  $E_a = 1000$  mV. Two anodic peaks,  $A_1$  and  $A_4$ , appear on sweeping the potential in the anodic direction. These peaks are related to the formation of  $\text{NiO}$  and  $\text{Ni}_2\text{O}_3$ , respectively.



On sweeping the potential in the cathodic direction only one cathodic peak  $C_4$  appears due to the reduction of  $\text{Ni}_2\text{O}_3$  to  $\text{NiO}$ . The cathodic  $C_1$ , which is mainly ascribed to the reduction of  $\text{NiO}$  to  $\text{Ni}$ , does not appear due to the transformation (on switching the potential at  $E_a$  of more noble values) of  $\text{NiO}$  to species, which are reduced at more negative potential [15].



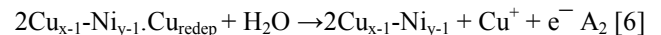
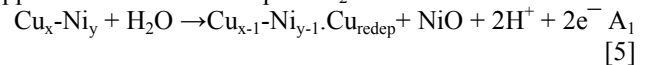
**Figure 1.** Cyclic voltammograms of (1) copper, (2) nickel, (3) alloy I, and (4) alloy II in 0.1 M  $\text{Na}_2\text{SO}_4$  at  $25^\circ\text{C}$  and scan rate  $50 \text{ mV s}^{-1}$

Figure 1, curves 3 and 4 represent the cyclic voltammetric behaviour of the alloys I and II, respectively. The cyclic voltammograms were characterized by the existence of well-defined potential regions (separated by a certain critical potential  $E_{\text{crit}}$ ); the subcritical or selective dissolution potential region and the simultaneous dissolution potential region. The zero current potential of the two alloys are situated at potentials more negative than those of pure copper and pure nickel.

### 3.1. The Subcritical Potential Region

It seems that the dissolution of the alloys in this region follow the dissolution – redeposition mechanism where both

copper and nickel dissolves initially followed by the redeposition of the more noble component, copper. This region was characterized by the appearance of the anodic peaks  $A_1$  and  $A_2$ . The anodic peak  $A_1$  represent the situation where both of copper and nickel dissolves followed by copper redeposition on the alloy surface and the oxidation of nickel to  $\text{NiO}$  and/ or  $\text{Ni(OH)}_2$ . It is seems that, taking into consideration the molar ratio of nickel in the alloy, the peak current density  $i_p$  of the peak  $A_1$  was increased on alloying nickel with copper. These results indicate the enhancement of the selective dissolution of nickel from the alloy with increasing the copper content. These results indicate that the dissolution of copper with nickel initially assists the diffusion of the nickel from the bulk of the alloy towards its surface and hence increases the peak current density of the anodic peak  $A_1$ . By thermodynamic reasoning, it can be shown that this process is impossible unless, in accordance with the principles of irreversible thermodynamics, a coupling between the anodic partial reactions occurs, which may reflect an average activity of adsorbed ad-atoms of the electropositive component  $\text{Cu}$  that exceeds unity [13]. If this situation prevails,  $\text{Cu}^+$  ions may be dissolved from the alloy at underpotentials that are cathodic with respect to the reversible potential  $E_{\text{Cu}}$ , that agglomerates on the electrode surface. They have, therefore, the character of an unstable intermediate species and will be plated out on the surface of  $\text{Cu}$  crystals at the same electrode potential, which leads to the appearance of the anodic peak  $A_2$  and formation of  $\text{CuO}$ .



### 3.2. Simultaneous Dissolution Potential Region

This region lies at potential nobler than the critical potential  $E_{\text{crit}}$  of the alloys, where simultaneous dissolution of both nickel and copper occur. The following observations can be made: (i) in alloy I (low nickel content) the surface losses its planarity and acquires the porous structure as shown by the hysteresis loop of the voltammogram on switching the potential in the cathodic direction and as seen from the SEM micrograph in Fig. 2. The formation of surface porous structure was reported [16] for an active  $\text{Ni}$  dissolution in  $\text{H}_2\text{SO}_4$  at potentials  $-0.25 \text{ V Ag/AgCl}$  by a step-flow mechanism, followed by the rapid formation of large three-dimensional etch pits, leading to considerable surface roughening. (ii) in alloy II (high nickel content) this region was characterized by the appearance of three anodic peaks  $A_3$  and  $A_4$  corresponding to the formation of  $\text{CuO}$  and  $\text{Ni}_2\text{O}_3$ , respectively. Figure 3 represent x-ray diffraction analysis of the layer formed on the surface of alloy I polarized to  $-100 \text{ mV}$  showed that this layer composes of  $\text{NiO}$ ,  $\text{Ni(OH)}_2$  and  $\text{Cu}_2\text{O}$ . The X-ray diffraction analysis of the layer formed on the surface of alloy II polarized to  $1000 \text{ mV}$  showed that this layer composes of  $\text{Ni}_2\text{O}_3$  and  $\text{CuO}$ , Fig. 4

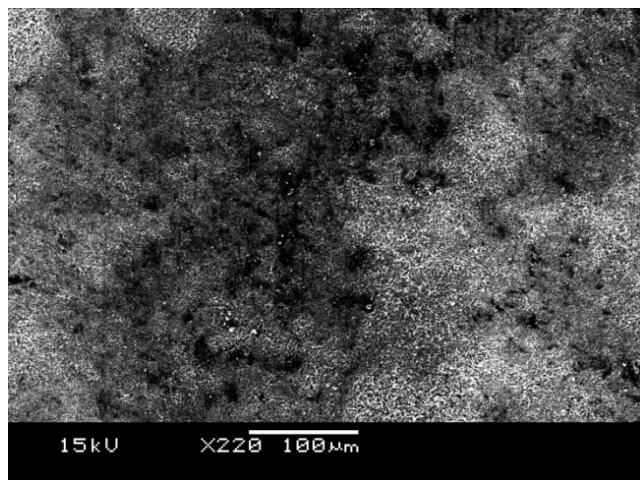


**Figure 2.** SEM micrograph of the alloy I surface after anodic polarization to 200 mV in 0.1 M Na<sub>2</sub>SO<sub>4</sub> at 25°C and scan rate 50 mV s<sup>-1</sup> (x220)

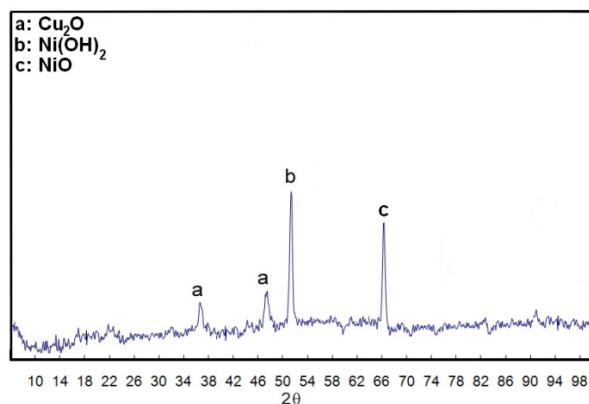


**Figure 3.** X-ray diffraction analyses of the surface of alloy I after anodic polarization to -100 mV in 0.1 M Na<sub>2</sub>SO<sub>4</sub> at 25°C

The complementary relationship between the anodic and cathodic peaks was studied by sweeping the potential from  $E_c = -1600$  mV and reversing it at different  $E_a$  values. Inspection of the data in the voltammogram of alloy I, Figs. 5 and 6 showed that on reversing  $E_a$  at value more noble than the potential of the anodic peak  $A_1$  two cathodic peaks  $C_1$  and  $C_2$  appear as a result of reduction of Ni(OH)<sub>2</sub> and NiO to Ni respectively. Reversing  $E_a$  at value more noble than the potential of the anodic peak  $A_2$  three cathodic peaks  $C_1$ ,  $C_2$  and  $C_3$  appear. The cathodic peak  $C_3$  is related to the reduction of Cu<sub>2</sub>O to Cu. On reversing  $E_a$  at value more noble than the potential of the anodic peak  $A_3$  four anodic peaks  $C_1$ ,  $C_2$ ,  $C_3$  and  $C_4$  appear. The cathodic peak  $C_4$  represents the reduction of CuO to Cu<sub>2</sub>O. On reversion the potential beyond the potential value of the anodic peak  $A_4$  a new cathodic peak,  $C_5$ , appears as a result of the reduction of Ni<sub>2</sub>O<sub>3</sub> to Ni<sup>+2</sup> compounds.

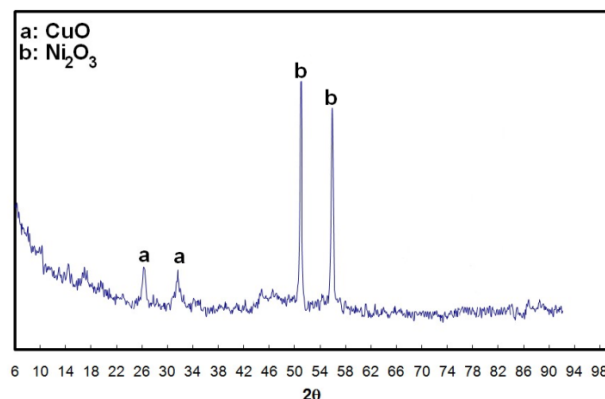


**Figure 4.** X-ray diffraction analyses of the surface of alloy II after anodic polarization to 700 mV in 0.1 M Na<sub>2</sub>SO<sub>4</sub> at 25°C

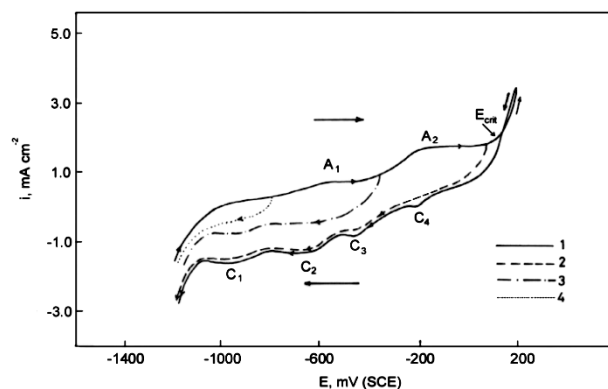


**Figure 5.** Cyclic voltammograms of alloy I in 0.1 M Na<sub>2</sub>SO<sub>4</sub> at 25°C, scan rate 50 mV s<sup>-1</sup> and various reversing anodic potentials: (1) -750 mV, (2) -400 mV, (3) 0.0 mV and (6) 200 mV

Figures. 7 and 8 show the influence of the sweep rate on the electrochemical behaviour of the alloys I and II, respectively. The general shapes of the voltammograms remained unchanged with increasing the sweep rate. It seems that, increasing the scan rate increases the peak current densities  $i_p$  of the anodic peaks and shifts their peak potentials  $E_p$  as well as the critical potential  $E_{crit}$  to more noble potentials. The voltammograms were used to analyze the dependence of peak current density  $i_p$  and peak potential  $E_p$  on the sweep rate. Figure 9 represents the linear dependence of the peak current density  $i_p$  of the anodic peaks on the root of the scan rate, where lines passing by origin was obtained for the anodic peaks  $A_2$ ,  $A_3$  and  $A_4$  (alloy II) or slightly different than zero for the peaks  $A_1$  and  $A_2$  (alloy I) and  $A_1$  (alloy II). The intercepts different than zero indicate that the induction rate is required before the electrode reactions become limited by diffusion. The linear dependence of the peak potential  $E_p$  of the anodic peaks  $A_1$ ,  $A_2$ ,  $A_3$  and  $A_4$  of alloy II and  $A_1$  of alloy I vs.  $\log v$  is given in Fig 10.

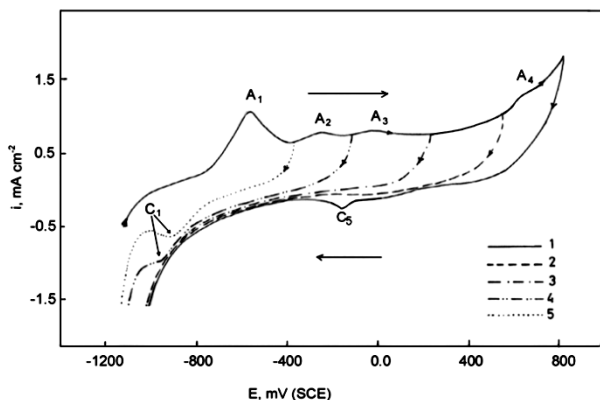


**Figure 6.** Cyclic voltammograms of alloy II in 0.1 M  $\text{Na}_2\text{SO}_4$  at 25°C, scan rate  $50 \text{ mV s}^{-1}$  and various reversing anodic potentials: (1) -400 mV, (2) -150 mV, (3) 200 mV, (4) 500 mV and (5) 800 mV

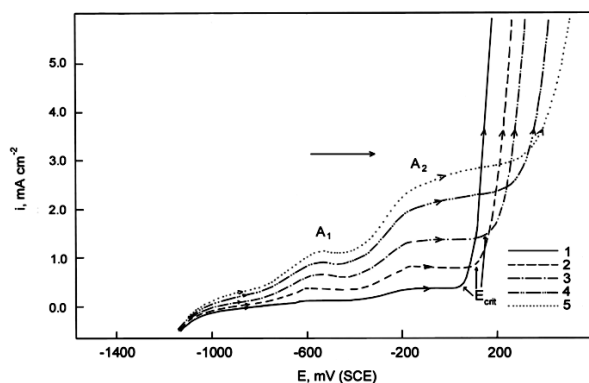


**Figure 7.** Potentiodynamic anodic polarization of alloy I in 0.1 M  $\text{Na}_2\text{SO}_4$  at 25°C and different scan rates: (1)  $10 \text{ mV s}^{-1}$ , (2)  $25 \text{ mV s}^{-1}$ , (3)  $50 \text{ mV s}^{-1}$ , (4)  $75 \text{ mV s}^{-1}$  and (5)  $100 \text{ mV s}^{-1}$

In order to obtain more information about the electrochemical behaviour of copper-nickel alloys in  $\text{Na}_2\text{SO}_4$  solution, potentiostatic current/time transients were carried out at different anodic step potentials,  $E_s$ . Figure 11 represents the current transients of alloy II in 0.1 M  $\text{Na}_2\text{SO}_4$ . It is seen that the current density decreases rapidly with time at first and then reaches a steady-state value. As the value of the potential is made more positive, both of the instantaneous and steady-state current values increase due to and increase in the thickness of the anodically formed layers. Plotting the current density vs.  $t^{-1/2}$  for the descending part of the current transients gives straight lines passing by the origin, Fig. 12. When  $E_s$  at -500 mV, there is two slopes as one could be expect, owing to the formation of two different layers, NiO and  $\text{Ni}(\text{OH})_2$ . If  $E_s$  is fixed at -200, 0.0 mV, the line consists of three portions with three different slopes due to the formation of three different layers (NiO,  $\text{Ni}(\text{OH})_2$  and  $\text{Cu}_2\text{O}$ ) with three different potentials. Four different layers with four different potentials NiO,  $\text{Ni}(\text{OH})_2$ ,  $\text{Cu}_2\text{O}$  and CuO are expected when  $E_s$  was fixed at 200 mV where a line with four portions with four different slopes. When  $E_s$  was fixed at 200 mV a line with five portions with five different slopes was obtained due to the formation of NiO,  $\text{Ni}(\text{OH})_2$ ,  $\text{Cu}_2\text{O}$ , CuO and  $\text{Ni}_2\text{O}_3$ . These linear relations support the suggestion that

the growth of the NiO,  $\text{Ni}(\text{OH})_2$ ,  $\text{Cu}_2\text{O}$ , CuO and  $\text{Ni}_2\text{O}_3$  layers are diffusion-controlled processes and obey the following equation [17,18] where  $P = z.c.D^{1/2}/\pi^{1/2}$ , where  $z$  is the number of exchanged electrons,  $c$  is the concentration of the electrolyte and  $D$  is the diffusion coefficient of the diffusing species.

$$i = P / t^{1/2}$$

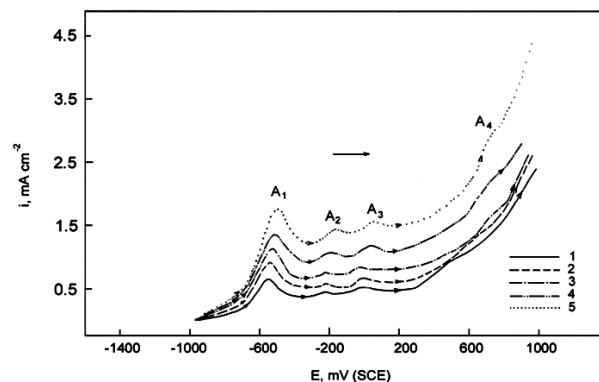


**Figure 8.** Potentiodynamic anodic polarization of alloy II in 0.1 M  $\text{Na}_2\text{SO}_4$  at 25°C and different scan rates: (1)  $10 \text{ mV s}^{-1}$ , (2)  $25 \text{ mV s}^{-1}$ , (3)  $50 \text{ mV s}^{-1}$ , (4)  $75 \text{ mV s}^{-1}$  and (5)  $100 \text{ mV s}^{-1}$

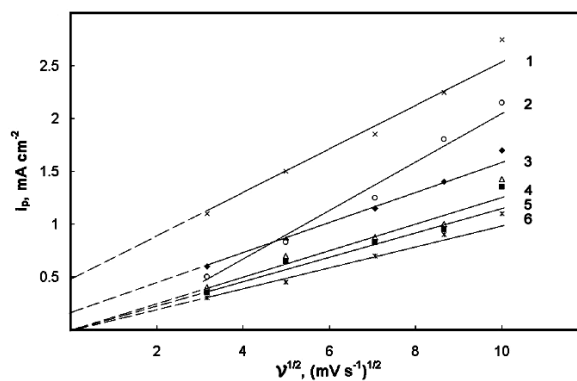


**Figure 9.** Relation between the peak current density,  $i_p$ , and the root of scan rate for the anodic peaks of: (1)  $A_1$  alloy I, (2)  $A_2$  alloy I, (3)  $A_1$  alloy II, (4)  $A_3$  alloy II, (5)  $A_2$  alloy II and (6)  $A_4$  alloy II

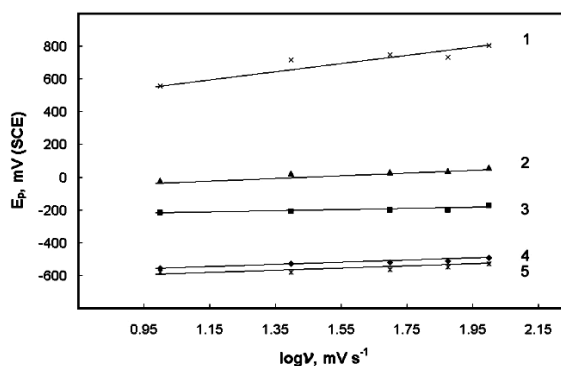


**Figure 10.** Relation between peak potential of the anodic peaks  $E_p$  and  $\log v$  in 0.1 M  $\text{Na}_2\text{CO}_3$  at 25°C of alloy II: (1)  $A_4$ , (2)  $A_3$ , (3)  $A_2$ , (4)  $A_1$  and of alloy I (5)  $A_1$

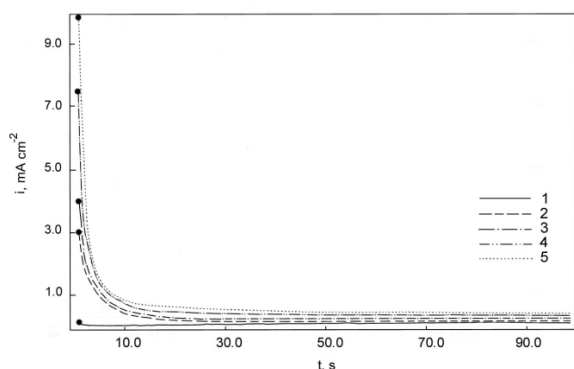


**Figure 11.** Current transients vs. time recorded for alloy II in 0.1 M  $\text{Na}_2\text{SO}_4$  at 25°C and constant anodic step potentials: (1)600 mV, (2)200 mV, (3) 0.0 mV, (4) -200 mV and (5) -500 mV

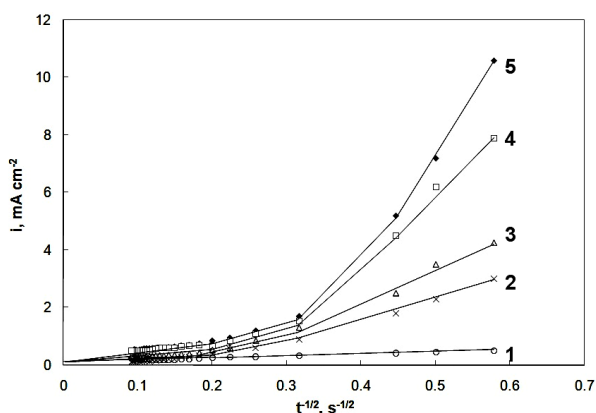


**Figure 12.** Dependence of the current density on  $t^{1/2}$  for the descending portions of the current transients for alloy II in 0.1 M  $\text{Na}_2\text{SO}_4$  at 25°C and constant anodic step potentials: (1)600 mV, (2)200 mV, (3) 0.0 mV, (4) -200 mV and (5) -500 mV

## 4. Conclusions

Two alloys of different composition are used to study the electrochemical behaviour of copper-nickel system sodium sulphate solutions using cyclic voltammetric, potentiodynamic anodic polarization and potentiostatic current time transient techniques.

The forward sweep was characterized by the appearance of two well-defined potential regions separated by the critical potential  $E_{\text{crit}}$ : the selective dissolution potential region and the simultaneous dissolution potential region.

The dissolution of the alloys in the first region follow the dissolution – redeposition mechanism where both copper and nickel dissolves initially followed by the redeposition of the more noble component, copper. This region was characterized by the appearance of the anodic peaks  $A_1$  and  $A_2$  where  $\text{Ni}(\text{OH})_2$  and  $\text{NiO}$ , and  $\text{CuO}$  are formed respectively.

The simultaneous potential region was characterized by surface enlargement and the appearance of two anodic peaks

$A_3$  and  $A_4$ , which are related to the formation of  $\text{Cu}_2\text{O}$  and  $\text{Ni}_2\text{O}_3$ , respectively.

The SEM micrograph showed surface enlargement and pits formation.

The reverse sweep was characterized by the appearance of five cathodic peaks  $C_5$ ,  $C_4$ ,  $C_3$ ,  $C_2$  and  $C_1$ , which are related to the reduction of  $\text{Ni}_2\text{O}_3$  to  $\text{Ni}^{+2}$  compounds,  $\text{CuO}$  to  $\text{Cu}_2\text{O}$ ,  $\text{Cu}_2\text{O}$  to  $\text{Cu}$ ,  $\text{NiO}$  to  $\text{Ni}$  and  $\text{Ni}(\text{OH})_2$  to  $\text{Ni}$ , respectively.

Potentiostatic current/time transient measurements reveal that the formation of  $\text{Ni}(\text{OH})_2$ ,  $\text{NiO}$ ,  $\text{Cu}_2\text{O}$ ,  $\text{CuO}$  and  $\text{Ni}_2\text{O}_3$  layers involves a nucleation and growth mechanism under diffusion control.

## REFERENCES

- [1] R. E. Reed-Hill and R. Abbaschian; Physical Metallurgy Principles, 3rd ed., PWS Publishing company, 20 Park Plaza, Boston, MA 02116-4324 (1994).
- [2] R. D. K. Misra and G. T. Burstein; J. Electrochem. Soc., 131 (1984) 1515.
- [3] R. D. K. Misra; Electrochim. Acta., 31 n. 1 (1986) 51.
- [4] A. E. Bohe, J. R. Vilche and A. J. Arvia, J. Appl. Electrochem., 20 (1990) 418.
- [5] W. K. Paik and Z. Szklarski-Smibwska; Surf. Sci., 96 (1980) 401.
- [6] A. M. Zaky, and F. H. Assaf, F. H., Br. Corros. J., 37, no. 1 (2002) 48.
- [7] A. M. Zaky, F. H. Assaf, S. S. Abd El Rehim, and B. M. Mohamed; Br. Corros. J., 37, no. 4 (2002) 311
- [8] A. E. Bohe, J. R. Vilche and A. J. Arvia; J. Appl. Electrochem, 14 (1984) 645.
- [9] K. J. Vetter; Electrochemical Kinetics, acadinic Press, New York (1967).
- [10] T. Vitanov, A. Popov and E. Budevski; J. Electrochem. Soc., 121 (1974) 207.
- [11] H. W. Pickering and C. Wagner, J. Electrochem. Soc., 114 (1967) 698.
- [12] H. W. Pickering, J. Electrochem. Soc., 117 (1970) 8.
- [13] H. Gerischer; in Korrosion XIV (Korrosionsschutz Durch Legieren, Verlag Chemie, Weiheim (1962).
- [14] M. Pourpaix, "Atlas of Electrochemical Equilibria in Aqueous Solutions", Pregamon Press, New York (1966).
- [15] W. Visscher and E. Barandrecht, Electrochim. Acta, 25 (1980) 651.
- [16] J. Scherer, B. M. Ocko and O.M. Magnussen; Electrochim. Acta 48 (2003) 1169.
- [17] J. B. Randles; Trans Faraday Soc., 44 (1948) 327.
- [18] A. Sevcik; Collect. Czech. Chem. Commun., 13 (1948) 349.